

Ferromagnetic

Subjects: Physics, Condensed Matter

Contributor: Ajaya Bhattarai, Nitin Sharma

Ferromagnetism is a phenomenon whereby a substance can become a permanent magnet or strongly reacts to a magnetic field.

Keywords: ferromagnetism ; external magnetic field ; intrinsic defect

1. Introduction

Ferromagnetism is a phenomenon whereby a substance can become a permanent magnet or strongly reacts to a magnetic field. The term “ferromagnetism” is derived from the magnetism detected in Fe^{2+} or Fe, as Fe was the first element in which ferromagnetism was observed [1]. Unlike nonmagnetic compounds, the compounds exhibiting ferromagnetism show the spontaneous parallel alignment of permanent dipoles due to the movement of electrons around atomic orbitals. Pierre-Ernest Weiss discovered the structural alignments of dipoles [2]. Although these alignments develop high magnetizations even in the absence of a magnetic field, they occur in microscopic spaces known as domains. As these domains do not possess alignments, the ferromagnetic compound does not, by itself, act as a magnet. However, upon exposure to an external magnetic field, these domains align in different directions and maintain themselves in a particular direction, creating a temporary magnetic field within the substance. In the absence of a magnetic field, the net magnetic field is significantly lower, approximately equal to zero. These domains of ferromagnetic elements have been investigated in the absence and presence of a magnetic field (**Figure 1a–d**).

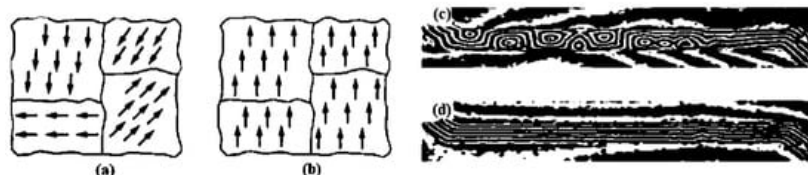


Figure 1. Alignments of magnetic domains in the absence and presence of a magnetic field. **(a,b)**: Alignment of the magnetic domain in the absence and presence of a magnetic field (Microsoft Bing), respectively. **(c,d)**: Images of the magnetic domain in the presence and absence of a magnetic field, respectively, acquired by a Lorentz electron microscope [3] (Published with permission of SPIE).

Naturally occurring elements, such as Co, Ni, and Fe, as well as the alloys formed by these elements and some metal and nonmetal oxides that demonstrate ferromagnetism, are termed as “ferromagnetic substances” [4]. The materials and elements exhibiting ferromagnetism can function within a certain temperature threshold known as the Curie temperature. When ferromagnetic substances are heated above the Curie temperature, they lose their ferromagnetic properties and become weakly magnetic, i.e., paramagnetic. This is because, at temperatures above the Curie temperature, the thermal energy is sufficient to break the internal alignments of domains. Below the Curie temperature, magnetism can be permanently induced in these materials. When ferromagnetic materials are subjected to constant external magnetic fields, the abovementioned phenomenon occurs as the magnetic domains are aligned in the same direction (**Figure 1b**). However, if these materials are exposed to external magnetic fields for prolonged durations, they become permanently magnetized [5].

2. Recent Trends

Conventionally used ferromagnetic materials exhibit some limitations, such as a low hardness, which hinders their application and has necessitated the development of better ferromagnetic materials [6]. When ferromagnetism was unexpectedly observed in Ge, Mn, and Te, several studies were conducted on inorganic nonmetallic materials, and many ferromagnetic materials were successfully discovered. Traditionally, ferromagnetism was believed to be demonstrated by elements with partially filled d or f orbitals. In contrast, when researchers revealed that an element without partially filled d

or f orbitals could also exhibit ferromagnetism, it opened up a completely new realm in the field of ferromagnetism. Reducing one of the dimensions limits the electronic transition, promoting column interactions and increasing the bandwidth ratio. This increase in material–column interactions and bandwidth ratio induces magnetism in these materials [7]. Numerous materials with either partially filled f or d orbitals were both theoretically and experimentally analyzed. Nonmagnetic elements that show ferromagnetism in their oxide compounds or other forms are referred to as d^0 ferromagnetic substances, and the corresponding ferromagnetism is termed d^0 ferromagnetism. d^0 Ferromagnetism was discovered for the first time in HfO_2 when the O-rich surface of Hf with no magnetic ions in HfO_2 exhibited ferromagnetism [8]. Thereafter, the ferromagnetic properties of oxides of other elements of the same period, including ZnO , Cu_2O , and TiO_2 , were examined, and these oxides were found to demonstrate ferromagnetism; furthermore, numerous other nonmagnetic d-block elements, such as Sc, Cr, Mn, Zr, and Nb, were reported to exhibit ferromagnetism upon doping with some specific type of impurities [9]. Similarly, oxides of f block elements, such as CeO_2 doped with Co and Mn, were investigated to further explore this [10]. Moreover, the oxides of nonmagnetic elements without d or f orbitals, including Al_2O_3 , In_2O_3 , and CaO , demonstrated ferromagnetic properties, implying that these properties can be modified within elements [11]. Subsequently, the non-oxide nonmagnetic compound BN, C structures, and rock salts were also reported to possess considerable ferromagnetism [12]. Accordingly, it was concluded that modification of the internal environment of a nonmagnetic element or a ferromagnetic nonmetal by defects, such as valency complexes, vacancies, and impurities, arising from the integration of the element with another element, can induce magnetic properties [13]. Thus, the phenomenon of ferromagnetism is universal, and is demonstrated not only by magnetic elements, but also their impurities and non-magnetic elements by doping with oxide or other inorganic elements [14]. Furthermore, the drawbacks that limit the use of traditional magnetic elements have been overcome by mixing these elements with other compounds; for example, B [6]. Many modern medical procedures, such as varicose treatment, hyperthermia, and endovenous thermal ablation require local heating of the human body. However, it is challenging to convert electrical power into heat flux and directly transfer this heat flux to the required area without harming the surrounding tissue. Heating catheters composed of biocompatible magnetic composites with low-frequency induction heating (LFIH) is an effective solution in this regard [15]. Cu–Mn–Ga-based ferromagnetic shape memory single crystals were fabricated for the first time by annealing their cast polycrystalline alloys. Their functional properties have also been reported. The obtained results should be highly significant for the development of brittle ferromagnetic Cu–Mn–Ga alloys [16]. Numerous studies have been performed on the advancement of ferromagnetism, which have resulted in the discovery of numerous ferromagnetic compounds.

2.1. Hexaborides of Alkaline-Earth Metals

Boride compounds are gaining considerable attention because of their mechanical properties and high conductivities. They are widely used to overcome the hardness limitations of magnetic elements [6]. B, as an electron-deficient element, facilitates the trapping of electrons from other metal species by forming a strong B bond with these species. They produce either divalent-metal hexaborides or divalent hexaborides with alkaline-earth metals [17]. The hexaborides of alkaline-earth metals, including SrB_6 , BaB_6 , and CaB_6 , are extremely sensitive to stoichiometry because of their high impurity contents and inferior physical properties. When these compounds were doped with Th and La, the resulting compounds demonstrated weak ferromagnetism at high temperatures [18]. Although these compounds lack d or f orbitals, their ferromagnetism has attracted significant research attention [9]. Divalent hexaborides (MB_6 , M = Sr, Ba, Ca) crystallize in CsCl-type cubic structures, and their physical properties are substantially similar to those of Group IIA elements, that is, alkaline-earth metals [19]. The structure of a divalent hexaboride comprises a central metal ion surrounded by hexaboride ions (**Figure 2**). In the CaB_6 prototype structure, a single metal atom is surrounded by eight octahedra of B atoms, each centered on the corner of the cube. There are five B atoms in an octahedron, with four adjacent atoms and one along one of its axes. Moreover, 24 B atoms are coordinated at the center of the atom; nevertheless, no valence bonds are formed between them [20]. In contrast, the B atoms are covalently bonded to each other and are responsible for several physical and chemical properties of these compounds [21]. A cubic B sublattice is inherently electron-deficient because the B atoms must distribute their three valence electrons over five bonds. This implies that a sublattice cannot exist, even with the donation of electrons from the metals. Hexaborides must contain a metal cation with a charge of at least +2 to be electronically stable [22]. KB_6 with a low K content has been synthesized in controlled environments [23]. Consequently, considering that the B sublattice forms a semi-rigid “cage,” alkaline-earth, rare-earth, and some actinide cations are the only candidates in this regard based on their sizes and valences.

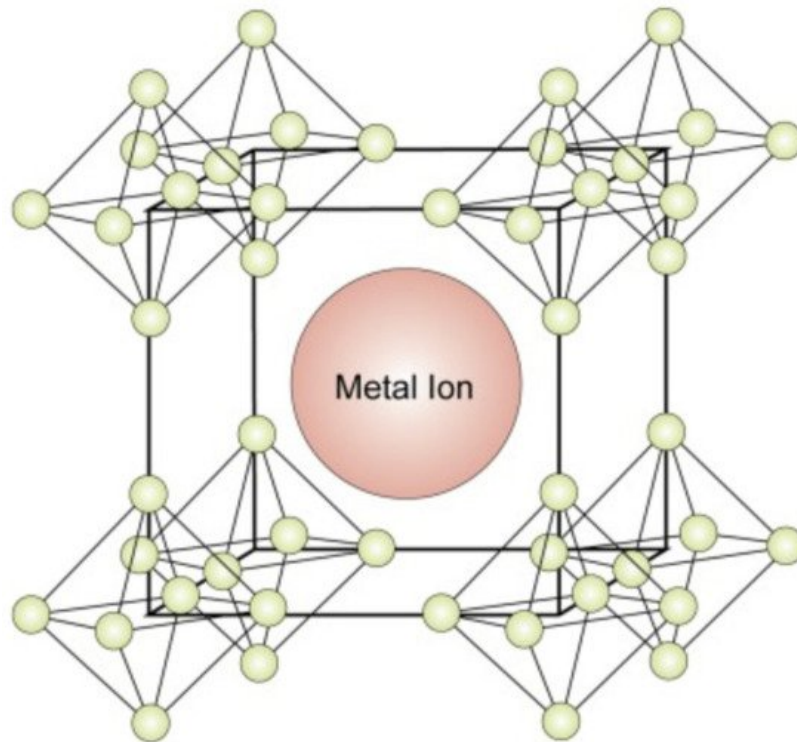


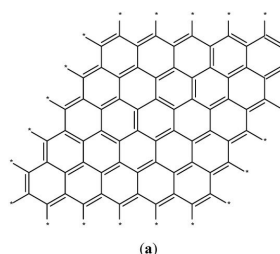
Figure 2. Crystal structure of the hexaborides of alkaline-earth metals [24].

2.2. Nonmagnetic Oxides

Numerous studies have been conducted on nonmagnetic oxides, and several other oxides of nonmetallic elements demonstrating ferromagnetism at room temperature have been discovered; nevertheless, there remains a knowledge gap regarding the origin of ferromagnetism in these compounds. Impurities and surface defects are the topic of controversies that are often discussed whenever the discussion arises [25]. Ferromagnetism has been discovered in different oxides, for example, Mg, Zn, Ce, Hf, Ti, Sr, Sn, and Zr oxides, disproving the traditional concept of the requirement of d or f orbitals to exhibit ferromagnetism. Among them, oxides of Zn, Mg, Hf, and Ce are widely used and have extensive applications, whereas the remaining oxides exhibit weak ferromagnetism in the free state or after doping [17].

2.3. C Nanostructures

Ferromagnetically active C systems have emerged as one of the most popular research topics in the field of ferromagnetism owing to their various advantages including low weight, high stability, low-cost production, and simple processing. Recent years have witnessed significant advancements using graphene (**Figure 3a**), C nanotubes (**Figure 3b**), fullerenes (**Figure 3c**), and graphite (**Figure 3d**) [26]. As classic ferromagnetic substances lack d and f orbitals, ferromagnetism in C nanostructures originates from s and p electrons. These nanostructures demonstrate ferromagnetism at low temperatures, and the magnetism is due to the impurities present in these nanostructures [27].



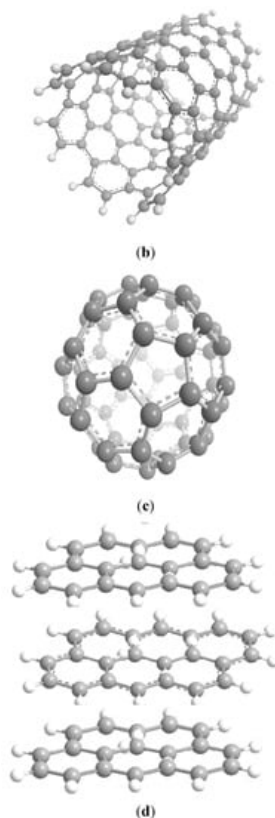


Figure 3. Schematics of the structures of graphene (a), C nanotubes (b), fullerenes (c), and graphite (d) [26].

2.4. Magnetic Boride Compounds

B has the potential to form a wide range of compounds with different electrochemical, magnetic, and stoichiometric properties. Magnetic elements are traditionally used for several applications; nevertheless, they exhibit some limitations such as a low hardness, which must be overcome using elements including B. The hardness of some elements, such as Fe, has been considerably increased by treatment with B [6]. Recent studies on B transition metal compounds have revealed improved mechanical properties for these compounds [28]. Due to the presence of unpaired d or f orbitals, magnetic properties such as high coercivity, high magnetization saturation, etc., can be greatly induced in magnetic boron compounds [29]. A superior magnetism is observed in metallic elements when they are incorporated with borides [30].

Metallic boride compounds including FeB, NiB, and Co_3B are intermediates between soft and hard magnets. Although they are magnetically hard, they possess low moments; hence, they are considered semi-hard compounds with immense application possibilities in various fields, for example, data storage and biomedicine [31]. However, very few studies have reported on the development of these compounds as compared to those for other classes of compounds.

2.5. Nonmetallic Non-Oxide System

Nonmetallic non-oxides, such as nitrides, are attracting interest for the induction of magnetization using various elements, similar to the cases of oxides. The magnetism in these compounds is caused by significant spin-exchange interactions in the ionic states. Nevertheless, it is highly useful to stabilize the hole carrier density for doping interactions. Localized acceptors can be utilized to stabilize the quantum confinement effect [32].

These classes of ferromagnetic compounds are specifically prepared from Group 3 and Group 5 elements, and the thicknesses of GaAs, GaN, InAs, and GaP are inversely proportional to their magnetic saturations; furthermore, these compounds can be fabricated using Group 4 elements such as Ge (for example, Mn^{2+} -doped Ge). In Group 4 element-based ferromagnetic compounds, ferromagnetism originates from Mn-induced charge carriers, that is, holes in the material matrix. Bound magnetic polarons (BMPs) are formed during exchange interaction between the magnetic dopant and localized holes. These BMPs are composed of magnetic ions and a localized hole, and the interaction of these BMPs in the presence of a high concentration of dopants leads to ferromagnetism [33]. However, at low temperatures, these BMPs overlap each other and interact with nearby dopants. Eventually, the alignment of these BMPs causes a ferromagnetic transition. Nevertheless, the resulting ferromagnetism is comparatively lesser than those of similar systems. Comparative studies of the saturation magnetizations, observations, and origins of ferromagnetism of different ferromagnetic materials are presented in **Table 1**.

Table 1. Comparative studies of the saturation magnetizations, observations, and origins of ferromagnetism of different ferromagnetic materials.

Materials	Saturation Magnetization (emu/g)	Observation	Origin of Ferromagnetism	References
Traditional materials				
Fe	217.9	Field-induced change in the magnetic domain	Interactions between electrons in the outermost d orbitals	[34]
Co	162.7	Field-induced change in the magnetic domain	Interactions between electrons in the outermost d orbitals	[34]
Ni	57.5	Field-induced change in the magnetic domain	Interactions between electrons in the outermost d orbitals	[34]
Magnetite (Fe_3O_4)	90.92	Less strongly magnetized than the parent materials	Magnetic domains of parent materials	[34][35]
Maghemite (Fe_2O_3)	84–88	Less strongly magnetized than the parent materials	-	[34]
CoFe_2O_4	~75	Although the parent materials are ferromagnetic, it shows less ferromagnetism	Magnetism of parent materials	[34]
Hexaborides of alkaline-earth metals				
CaB_6 films	Thickness: 0.5 μm (~4.63) Thickness: 1.6 μm (~0.46) Thickness: 2.3 μm (~0.102)	Saturation magnetization is inversely proportional to thickness	Defects induced by grains boundaries and lattice distortion	[36]
CaB_6 crystals	~0.0489	Samples demonstrated ferromagnetism	Surface contamination	[37]
BaB_6 thin films	~2.454 at 450–550 $^{\circ}\text{C}$	No variation due to thickness	Surface contamination	[9]
SrB_6	0.06 μ_{B} per unit cell	Temperature affected the magnetic properties	Defects of surface layers	[38]
Nonmagnetic oxides				
HfO_2 films	~13.223	Annealing and vacuuming influenced ferromagnetism	Porous structure of the film O vacancies	[39]
ZnO thin films	annealed at 150 $^{\circ}\text{C}$: 0.08 annealed at 600 $^{\circ}\text{C}$: 0.42 (at 300 K)	Thermal annealing under an Ar flow caused a defect	Single occupied O vacancies	[40]
ZnO nanowires	0.41 at 300 K	Structural elongation was determined by an applied parallel magnetic field	2p orbitals of O; when Zn affects the local spin moment of the O orbital	[30]
ZnO films doped with K	0%K-doped ZnO films: 0.79 4%K-doped ZnO films: 1.09 6%K-doped ZnO films: 1.3 8%K-doped ZnO films: 1.91 11%K-doped ZnO films: 0.63 (at $T = 300$ K)	With an increase in the K concentration, the saturation magnetization initially increased and then decreased	Holes and ZnK defect	[41]

Materials	Saturation Magnetization (emu/g)	Observation	Origin of Ferromagnetism	References
ZnO nanoparticles (NPs)	Raw NPs: Diamagnetic 50 h-milled NPs: 0.031 100 h-milled NPs: 0.047 200 h-milled NPs: 0.086 (at $T = 300$ K)	Mechanical milling of diamagnetic ZnO powders induced defects. With an increase in the defect concentration, ferromagnetism increased	Intrinsic defects related to O and Zn vacancies	[42]
	500 °C-sintered: 0.0183 850 °C-sintered: 0.0190 1300 °C-sintered: 0.00188 (at $T = 300$ K)	With an increase in temperature, the saturation magnetization initially increased and then again decreased	-Interstitial (Zn/O) ion defects in the samples	[43]
ZnO single crystals	0.63×10^{-4} (untreated sample) 0.16×10^{-3} (treated sample) ($T = 300$ K)	With an increase in the purity of the sample, the saturation magnetization increased	O vacancies generated by thermal annealing under an Ar flow	[30]
TiO ₂ films on Si substrates	PO ₂ = 50 mTorr: Diamagnetic PO ₂ = 0.2 mTorr: Very weakly Diamagnetic + FM (~0.005 PO ₂ = 0.02 mTorr: ~0.075 (At $T = 25$ °C)	The magnetic moment of the system was inversely proportional to the concentration of O vacancies	O vacancies	[44]
TiO ₂ films	Anatase film: ~0.52 Rutile film: ~1.42	Using vacuum, O vacancies can be filled	- Rutile films demonstrated ferromagnetism owing to O vacancies	[45]
Anatase TiO ₂ (12 h H ₂ -annealed to 873 K)	0.066	Hydrogenation generated local 3d moments	Complexes of Ti ³⁺ and O defects Hybridization of O vacancies with Ti 3d–O 2p orbitals	[46]
Transition metal ion (TM = Cr, Mn, Fe, Co, Ni, Cu)-doped rutile TiO ₂ single crystals	Undoped TiO ₂ : 0.00016 Cr-doped TiO ₂ : 0.00036 Mn-doped TiO ₂ : 0.00055 Fe-doped TiO ₂ : 0.00136 Co-doped TiO ₂ : 0.00021 Ni-doped TiO ₂ : 0.00086 Cu-doped TiO ₂ : 0.00015	Results suggest a close superposition of paramagnetic and ferromagnetic behaviors	Separation of the metallic phases of Ni, Co, and Fe Unpaired d electrons of transition metal ions	[47]
CeO _{2-x} films	When $x = 0.03$: ~1.34 When $x = 0.1$: ~1.02 ($T = 300$ K)	Both Ce ³⁺ and Ce ⁴⁺ are present	O and Ce vacancies	[48]
MgO films	Untreated sample: ~0.751 Annealed sample: ~0.329	Reduction in the concentration of Mg vacancies is proportional to the reduction of Mg after annealing	Mg cation vacancies	[49]
ZrO ₂ with Fe	205.56	Analysis helped to improve the magnetic characteristics of this system	Induced defects and stress	[50]

Materials	Saturation Magnetization (emu/g)	Observation	Origin of Ferromagnetism	References
High-purity SnO ₂ powders	0 h-milled: 0.0006 4 h-milled: 0.0019 12 h-milled: 0.0055 20 h-milled: 0.0105	Temperature increases inversely with saturation magnetization	Singly charged O vacancies High defect density -	[51]
SnO ₂ NPs	Powder in raw form: 0.019 Powder annealed at 773 K: 0.015 Powder annealed at 973 K: 0.012 Powder annealed at 1173 K: 0.010 Powder annealed at 1373 K: 0.006 Powder annealed at 1573 K: 0.001 (T = 300 K)	The saturation magnetizations of NPs reduced when the NPs were annealed at temperatures higher than 500 °C	O vacancies (T = 5 K)	[52]
Carbon Nanostructures				
Highly oriented graphite samples	Kish graphite: $0.6 \times 10^{-3} \pm 0.2 \times 10^{-3}$ at T = 300 K	Different possibilities for the ferromagnetic-like behaviors in the samples	Magnetic impurities Topological defects Itinerant ferromagnetism	[53]
C ₆₀	0.045 (T-A= πr 2527 °C) A= πr^2	Upon applying a pressure of 9 GPa at 800 K, the ferromagnetic behavior significantly decreased	C radical formation	[54]
Graphene	Annealing at T = 300 °C At 300 K: 0.004 At 2 K: 0.25 Annealing at T = -500 °C At 300 K: 0.020 At 2 K: 0.90	Graphene prepared at 1073 K did not clearly exhibit ferromagnetism	Defects induced by annealing	[27]
Graphene nanoribbons	1.1	Optimization of density twist and turn edge defects	Defect density	[55]
Implantation of ions on pyrolytic graphite—12C	14.4	Implantation steps are directly proportional to the vacancy density	Vacancy density	[56]
C Nanotubes	0.5227	N ₂ plasma treatment	Amine- and N pyridine-based bonding configuration	[57]
Magnetic Borides				
Ni ₂ B with O	29	Treatment of Ni with boride prevented the oxidation of Ni	Intrinsic defects -	[58]
CoB	75–135	Change in magnetic properties with an increase in crystallization	Intrinsic defects	[59]

References

- Chikazumi, S.; Graham, C.D. Physics of Ferromagnetism 2e (No. 94); Oxford University Press: Oxford, UK, 2009.

2. Cullity, B.D.; Graham, C.D. *Introduction to Magnetic Materials*, 2nd ed.; Wiley: New York, NY, USA, 2008.
3. Peng, L.-C.; Zhang, Y.; Zuo, S.-L.; He, M.; Cai, J.-W.; Wang, S.-G.; Wei, H.-X.; Li, J.-Q.; Zhao, T.-Y.; Shen, B.-G. Lorentz transmission electron microscopy studies on topological magnetic domains. *Chin. Phys. B* 2018, 27, 066802.
4. Goldman, A. *Handbook of Modern Ferromagnetic Materials*; Springer Science & Business Media: Berlin/Heidelberg, Germany, 2012.
5. Hashmi, S. *Comprehensive Materials Processing*; Elsevier: Amsterdam, The Netherlands, 2014.
6. Zhao, X.; Li, L.; Bao, K.; Zhu, P.; Tao, Q.; Ma, S.; Liu, B.; Ge, Y.; Li, D.; Cui, T. Synthesis and characterization of a strong ferromagnetic and high hardness intermetallic compound Fe₂B. *Phys. Chem. Chem. Phys.* 2020, 22, 27425–27432.
7. Singh, R. Unexpected magnetism in nanomaterials. *J. Magn. Magn. Mater.* 2013, 346, 58–73.
8. Das Pemmaraju, C.; Sanvito, S. Ferromagnetism Driven by Intrinsic Point Defects in HfO₂. *Phys. Rev. Lett.* 2005, 94, 217205.
9. Mohanta, S.K.; Mishra, S.N. Electronic structure and magnetic moment of dilute transition metal impurities in semi-metallic CaB₆. *J. Magn. Magn. Mater.* 2017, 444, 349–353.
10. Sundaresan, A.; Bhargavi, R.; Rangarajan, N.; Siddesh, U.; Rao, C.N.R. Ferromagnetism as a universal feature of nanoparticles of the otherwise nonmagnetic oxides. *Phys. Rev. B* 2006, 74, 161306.
11. Coey, J.M.D. Magnetism in d₀ oxides. *Nat. Mater.* 2019, 18, 652–656.
12. Zhang, J.; Gao, D.; Si, M.; Zhu, Z.; Yang, G.; Shi, Z.; Xue, D. Origin of the unexpected room temperature ferromagnetism: Formation of artificial defects on the surface in NaCl particles. *J. Mater. Chem. C* 2013, 1, 6216–6222.
13. Makarova, T.L. Nanomagnetism in otherwise nonmagnetic materials. *arXiv* 2009, arXiv:0904.1550.
14. Sundaresan, A.; Rao, C.N.R. Ferromagnetism as a universal feature of inorganic nanoparticles. *Nano Today* 2009, 4, 96–106.
15. Xiang, Z.; Le, M.Q.; Cottinet, P.-J.; Griffiths, P.; Baeza, G.P.; Capsal, J.-F.; Lermusiaux, P.; Della Schiava, N.; Ducharne, B. Development of anisotropic ferromagnetic composites for low-frequency induction heating technology in medical applications. *Mater. Today Chem.* 2021, 19, 100395.
16. Yang, S.; Li, M.; Qing, X.; Guo, L.; Hong, S.; Wang, L.; Wang, C.; Liu, X. Development of Cu-Mn-Ga-based ferromagnetic shape memory single crystals. *Materialia* 2020, 12, 100789.
17. Lungu, I.I.; Grumezescu, A.M.; Fleaca, C. Unexpected Ferromagnetism—A Review. *Appl. Sci.* 2021, 11, 6707.
18. Young, D.P.; Hall, D.; Torelli, M.E.; Fisk, Z.; Sarrao, J.L.; Thompson, J.D.; Ott, H.-R.; Oseroff, S.B.; Goodrich, R.G.; Zysler, R. High-temperature weak ferromagnetism in a low-density free-electron gas. *Nature* 1999, 397, 412–414.
19. Denlinger, J.D.; Clack, J.A.; Allen, J.W.; Gweon, G.-H.; Poirier, D.M.; Olson, C.G.; Sarrao, J.L.; Bianchi, A.D.; Fisk, Z. Bulk Band Gaps in Divalent Hexaborides. *Phys. Rev. Lett.* 2002, 89, 157601.
20. Schmidt, K.M.; Jaime, O.; Cahill, J.T.; Edwards, D.; Mixture, S.T.; Graeve, O.A.; Vasquez, V.R. Surface termination analysis of stoichiometric metal hexaborides: Insights from first-principles and XPS measurements. *Acta Mater.* 2018, 144, 187–201.
21. Etourneau, J.; Mercurio, J.-P.; Hagenmuller, P. Compounds Based on Octahedral B₆ Units: Hexaborides and Tetraborides. In *Boron and Refractory Borides*; Springer: Berlin/Heidelberg, Germany, 1977; pp. 115–138.
22. Johnson, R.W.; Daane, A.H. Electron Requirements of Bonds in Metal Borides. *J. Chem. Phys.* 1963, 38, 425.
23. Katsura, Y.; Yamamoto, A.; Ogino, H.; Horii, S.; Shimoyama, J.-I.; Kishio, K.; Takagi, H. On the possibility of MgB₂-like superconductivity in potassium hexaboride. *Phys. C Supercond. Its Appl.* 2010, 470, S633–S634.
24. Cahill, J.T.; Graeve, O.A. Hexaborides: A review of structure, synthesis and processing. *J. Mater. Res. Technol.* 2019, 8, 6321–6335.
25. Muñoz, M.C.; Gallego, S.; Sanchez, N. Surface ferromagnetism in non-magnetic and dilute magnetic oxides. *J. Phys. Conf. Ser.* 2011, 303, 012001.
26. Janani, M.; Srikrishnarka, P.; Nair, S.V.; Nair, A.S. An in-depth review on the role of carbon nanostructures in dye-sensitized solar cells. *J. Mater. Chem. A* 2015, 3, 17914–17938.
27. Wang, Y.; Huang, Y.; Song, Y.; Zhang, X.; Ma, Y.; Liang, J.; Chen, Y. Room-Temperature Ferromagnetism of Graphene. *Nano Lett.* 2009, 9, 220–224.
28. Mohammadi, R.; Lech, A.T.; Xie, M.; Weaver, B.E.; Yeung, M.T.; Tolbert, S.H.; Kaner, R.B. Tungsten tetraboride, an inexpensive superhard material. *Proc. Natl. Acad. Sci. USA* 2011, 108, 10958–10962.

29. Tang, C.; Ostrikov, K.; Sanvito, S.; Du, A. Prediction of room-temperature ferromagnetism and large perpendicular magnetic anisotropy in a planar hypercoordinate FeB₃ monolayer. *Nanoscale Horiz.* 2021, 6, 43–48.
30. Singh, V.; Ram, S.; Srinivas, V. Ferromagnetic nickel filled in borate shell by controlled oxidation–crystallization of boride in air. *J. Alloys Compd.* 2014, 610, 100–106.
31. Zieschang, A.-M.; Bocarsly, J.D.; Schuch, J.; Reichel, C.V.; Kaiser, B.; Jaegermann, W.; Seshadri, R.; Albert, B. Magnetic and Electrocatalytic Properties of Nanoscale Cobalt Boride, Co₃B. *Inorg. Chem.* 2019, 58, 16609–16617.
32. Peng, H.; Xiang, H.J.; Wei, S.-H.; Li, S.-S.; Xia, J.-B.; Li, J. Origin and Enhancement of Hole-Induced Ferromagnetism in First-Row d⁰ Semiconductors. *Phys. Rev. Lett.* 2009, 102, 017201.
33. Kaminski, A.; Das Sarma, S. Polaron Percolation in Diluted Magnetic Semiconductors. *Phys. Rev. Lett.* 2002, 88, 247202.
34. Schwerdt, J.I.; Goya, G.F.; Calatayud, M.P.; Herenu, C.B.; Reggiani, P.C.; Goya, R.G. Magnetic field-assisted gene delivery: Achievements and therapeutic potential. *Curr. Gene Ther.* 2012, 12, 116–126.
35. Nedelkoski, Z.; Kepaptsoglou, D.; Lari, L.; Wen, T.; Booth, R.A.; Oberdick, S.D.; Galindo, P.L.; Ramasse, Q.M.; Evans, R.F.L.; Majetich, S.; et al. Origin of reduced magnetization and domain formation in small magnetite nanoparticles. *Sci. Rep.* 2017, 7, 45997.
36. Zhao, G.; Zhang, L.; Hu, L.; Yu, H.; Min, G.; Yu, H. Structure and magnetic properties of nanocrystalline CaB₆ films deposited by magnetron sputtering. *J. Alloys Compd.* 2014, 599, 175–178.
37. Bennett, M.C.; van Lierop, J.; Berkeley, E.M.; Mansfield, J.F.; Henderson, C.; Aronson, M.C.; Young, D.P.; Bianchi, A.; Fisk, Z.; Balakirev, F.; et al. Weak ferromagnetism in CaB₆. *Phys. Rev. B* 2004, 69, 132407.
38. Cen, C.; Ma, Y.; Wang, Q.; Eom, C.-B. Surface magnetism and proximity effects in hexaboride thin films. *Appl. Phys. Lett.* 2017, 110, 102404.
39. Qi, L.-Q.; Han, R.-S.; Liu, L.-H.; Sun, H.-Y. Preparation and magnetic properties of DC-sputtered porous HfO₂ films. *Ceram. Int.* 2016, 42, 18925–18930.
40. Zhan, P.; Wang, W.; Liu, C.; Hu, Y.; Li, Z.; Zhang, Z.; Zhang, P.; Wang, B.; Cao, X. Oxygen vacancy–induced ferromagnetism in un-doped ZnO thin films. *J. Appl. Phys.* 2012, 111, 033501.
41. Liu, Y.; Zhou, W.; Huang, Y.; Wu, P. Unexpected ferromagnetism in n-type polycrystalline K-doped ZnO films prepared by RF-magnetron sputtering. *J. Mater. Sci. Mater. Electron.* 2015, 26, 8451–8455.
42. Phan, T.-L.; Zhang, Y.D.; Yang, D.S.; Nghia, N.X.; Thanh, T.D.; Yu, S.C. Defect-induced ferromagnetism in ZnO nanoparticles prepared by mechanical milling. *Appl. Phys. Lett.* 2013, 102, 072408.
43. Das, J.; Pradhan, S.K.; Mishra, D.K.; Sahu, D.R.; Sarangi, S.; Varma, S.; Nayak, B.B.; Huang, J.-L.; Roul, B.K. Unusual ferromagnetism in high purity ZnO sintered ceramics. *Mater. Res. Bull.* 2011, 46, 42–47.
44. Rumaiz, A.K.; Ali, B.; Ceylan, A.; Boggs, M.; Beebe, T.; Ismat Shah, S. Experimental studies on vacancy induced ferromagnetism in undoped TiO₂. *Solid State Commun.* 2007, 144, 334–338.
45. Kim, D.; Hong, J.; Park, Y.R.; Kim, K.J. The origin of oxygen vacancy induced ferromagnetism in undoped TiO₂. *J. Phys. Condens. Matter* 2009, 21, 195405.
46. Singhal, R.K.; Kumar, S.; Kumari, P.; Xing, Y.T.; Saitovitch, E. Evidence of defect-induced ferromagnetism and its “switch” action in pristine bulk TiO₂. *Appl. Phys. Lett.* 2011, 98, 092510.
47. Sangaletti, L.; Mozzati, M.C.; Galinetto, P.; Azzoni, C.B.; Speghini, A.; Bettinelli, M.; Calestani, G. Ferromagnetism on a paramagnetic host background: The case of rutile TM:TiO₂ single crystals (TM = Cr, Mn, Fe, Co, Ni, Cu). *J. Phys. Condens. Matter* 2006, 18, 7643–7650.
48. Fernandes, V.; Mossaneck, R.J.O.; Schio, P.; Klein, J.J.; De Oliveira, A.J.A.; Ortiz, W.A.; Mattoso, N.; Varalda, J.; Schreiner, W.H.; Abbate, M.; et al. Dilute-defect magnetism: Origin of magnetism in nanocrystalline CeO₂. *Phys. Rev. B* 2009, 80, 035202.
49. Mahadeva, S.K.; Fan, J.; Biswas, A.; Sreelatha, K.S.; Belova, L.; Rao, K.V. Magnetism of Amorphous and Nano-Crystallized Dc-Sputter-Deposited MgO Thin Films. *Nanomaterials* 2013, 3, 486–497.
50. Geng, K.; Xie, Y.; Xu, L.; Yan, B. Structure and magnetic properties of ZrO₂-coated Fe powders and Fe/ZrO₂ soft magnetic composites. *Adv. Powder Technol.* 2017, 28, 2015–2022.
51. Shi, S.; Gao, D.; Xu, Q.; Yang, Z.; Xue, D. Singly-charged oxygen vacancy-induced ferromagnetism in mechanically milled SnO₂ powders. *RSC Adv.* 2014, 4, 45467–45472.
52. Mehraj, S.; Ansari, M.S.; Al-Ghamdi, A.A. Alimuddin Annealing dependent oxygen vacancies in SnO₂ nanoparticles: Structural, electrical and their ferromagnetic behavior. *Mater. Chem. Phys.* 2016, 171, 109–118.

53. Guevenilir, E.; Kincal, C.; Kamber, U.; Guerlue, O.; Yildiz, D.; Grygiel, C.; Van der Beek, C.J. Investigation of ferromagnetism on graphite due to swift heavy ion irradiation. *Verh. Dtsch. Phys. Ges.* 2017, 50, 50004365.
54. Wood, R.A.; Lewis, M.H.; Lees, M.R.; Bennington, S.M.; Cain, M.G.; Kitamura, N. Ferromagnetic fullerene. *J. Phys. Condens. Matter* 2002, 14, L385–L391.
55. Sahu, V.; Maurya, V.K.; Singh, G.; Patnaik, S.; Sharma, R.K. Enhanced ferromagnetism in edge enriched holey/lacey reduced graphene oxide nanoribbons. *Mater. Des.* 2017, 132, 295–301.
56. Hühne, R.; Esquinazi, P. Can Carbon Be Ferromagnetic? *Adv. Mater.* 2002, 14, 753.
57. Fang, Z.; Zhao, H.; Xiong, L.; Zhang, F.; Fu, Q.; Ma, Z.; Xu, C.; Lin, Z.; Wang, H.; Hu, Z.; et al. Enhanced ferromagnetic properties of N₂ plasma-treated carbon nanotubes. *J. Mater. Sci.* 2019, 54, 2307–2314.
58. Singh, V.; Srinivas, V. Evolution of Ni:B₂O₃ core-shell structure and magnetic properties on devitrification of amorphous NiB particles in air. *J. Appl. Phys.* 2009, 106, 053910.
59. Yiping, L.; Hadjipanayis, G.C.; Sorensen, C.M.; Klabunde, K.J. Magnetic and structural properties of ultrafine Co-B particles. *J. Magn. Magn. Mater.* 1989, 79, 321–326.

Retrieved from <https://encyclopedia.pub/entry/history/show/53924>